Received: 5 June 2021 | Accepted: 6 September 2021

DOI: 10.1002/pamm.202100025

Fully Implicit RUNGE-KUTTA Schemes for Ideal Elastoplasticity

Bettina Schröder[1,*] and **Detlef Kuhl**[1,**]

[1] Institute of Mechanics and Dynamics, University of Kassel, Mönchebergstraße 7, 34109 Kassel

The present paper derives a multifield formulation of ideal elastoplasticity to enable the consistent application of higher order accurate RUNGE-KUTTA schemes. With the help of an axisymmetric model problem the appearing time discretization errors of distinct schemes are determined and compared.

1 Motivation

Industrial manufacturing strategies are often characterized by high speed process steps where dynamic effects within plastic deformations can't be neglected any longer, cf. [5]. Hence, the application of high order time discretization schemes and the assessment of corresponding errors are of great importance. A first step in that direction is the reformulation of plasticity as a multifield problem.

2 The Principle of JOURDAIN for Dynamic Ideal Elastoplasticity

The principle of JOURDAIN for dissipative continua is based on the stationarity of the balance of energy

$$\underset{\dot{\boldsymbol{u}},\dot{\boldsymbol{\varepsilon}}_\mathrm{p}}{\mathrm{stat}}\ \underset{\boldsymbol{\sigma}}{\sup}\ \underset{\gamma\geq 0}{\inf}\ P(\dot{\boldsymbol{u}},\ddot{\boldsymbol{u}},\dot{\boldsymbol{\varepsilon}}_\mathrm{p},\boldsymbol{\varepsilon}_\mathrm{p},\boldsymbol{\sigma},\gamma) \qquad \text{with} \qquad P=\dot{K}+\dot{E}+P^*+D. \tag{1}$$

Equation (1) consists of the rate of kinetic energy K, the rate of internal energy E, the power of external loads P^* and the pseudopotential D characterizing plastic effects, cf. [2, 4]. It furthermore depends on the stress tensor $\boldsymbol{\sigma}$, the plastic multiplicator γ, the displacement vector $\boldsymbol{u}$, the plastic strain tensor $\boldsymbol{\varepsilon}_\mathrm{p}$ as well as on corresponding first and second time derivatives. Evaluating Equation (1), performing a spatial discretization, and applying a semi-smooth NEWTON method yields the linearized semidiscrete form

$$\mathbf{M}\Delta\ddot{\mathbf{w}}+\mathbf{D}\Delta\dot{\mathbf{w}}+\mathbf{K}_1\Delta\mathbf{w}=\mathbf{R}_1^*-\mathbf{R}_1, \qquad \mathbf{K}_2\Delta\mathbf{w}=-\mathbf{R}_2, \qquad \gamma^{i,k+1}=0 \quad \forall i\in\mathcal{I}^k, \tag{2}$$

$$\mathcal{A}^{k+1}:=\{i|\gamma^{i,k+1}+d\,r_2^{i,k+1}>0\}, \quad \mathcal{I}^{k+1}:=\{i|\gamma^{i,k+1}+d\,r_2^{i,k+1}\leq 0\}.$$

Therein the vector of unknowns $\mathbf{w}=[\boldsymbol{u},\boldsymbol{\varepsilon}_\mathrm{p},\boldsymbol{\sigma},\gamma]$, the generalized mass matrix $\mathbf{M}$, the generalized damping matrix $\mathbf{D}$, the generalized stiffness matrices $\mathbf{K}_1,\mathbf{K}_2$, the generalized residual load vectors $\mathbf{R}_1,\mathbf{R}_2$, the external load vector $\mathbf{R}_1^*$ and the inactive as well as active set $\mathcal{I},\mathcal{A}$ are included. Moreover, $r_2^{i,k+1}$ represents the nodal evaluation i of the VON MISES yield function at iteration $k+1$ and $d\geq 0$ an arbitrary constant, cf. [3, 4].

3 RUNGE-KUTTA Schemes in Multifield Plasticity

For a temporal solution of Equation (2) higher order stiffly accurate fully implicit RUNGE-KUTTA integrators can be applied. Therefore, the time interval of interest $[0,T]$ is split into time steps $\Delta t=t_{n+1}-t_n$ and the stages $t_{ni}=t_n+c_i t_{ni}$ with $c_i\in[0,1]$ and $i=1,..,s$ are introduced. At the latter points in time Equation (2) is solved simultaneously. Therefore, the link

$$\mathbf{w}_\mathrm{t}=\mathbf{w}_{\mathrm{t},n}+\Delta t\mathbf{A}_\mathrm{t}\dot{\mathbf{w}}_\mathrm{t} \qquad \text{with} \qquad \mathbf{A}_\mathrm{t}=\begin{bmatrix} a_{11} & \cdots & a_{11} & a_{12} & \cdots & a_{12} & \cdots & a_{1s} & \cdots & a_{1s} \\ a_{21} & \cdots & a_{21} & a_{22} & \cdots & a_{22} & \cdots & a_{2s} & \cdots & a_{2s} \\ \vdots & \ddots & \vdots & \vdots & \ddots & \vdots & \cdots & \vdots & \ddots & \vdots \\ a_{s1} & \cdots & a_{s1} & a_{s2} & \cdots & a_{s2} & \cdots & a_{ss} & \cdots & a_{ss} \end{bmatrix}, \tag{3}$$

is established, whereby the matrix $\mathbf{A}_\mathrm{t}$ represents an extension of the RUNGE-KUTTA coefficients a_{ij}, cf. [1]. Furthermore, the stage values are aggregated in the vector $\mathbf{w}_\mathrm{t}=[\mathbf{w}_{n1},...,\mathbf{w}_{ns}]$, the corresponding time derivatives in $\dot{\mathbf{w}}_\mathrm{t}$ and the vector $\mathbf{w}_{\mathrm{t},n}$ consists of s copies of $\mathbf{w}_n$. Inserting the linearization of Relation (3) into Equation (2), yields the linear system of equations

$$\left[\frac{1}{\Delta t^2}\mathbf{M}_\mathrm{t}\mathbf{A}_\mathrm{t}^{-1}\mathbf{A}_\mathrm{t}^{-1}+\frac{1}{\Delta t}\mathbf{D}_\mathrm{t}\mathbf{A}_\mathrm{t}^{-1}+\mathbf{K}_{1,\mathrm{t}}\right]\Delta\mathbf{w}_\mathrm{t}=\mathbf{R}_{1,\mathrm{t}}^*-\mathbf{R}_{1,\mathrm{t}}, \qquad \mathbf{K}_{2,\mathrm{t}}\Delta\mathbf{w}_\mathrm{t}=-\mathbf{R}_{2,\mathrm{t}}, \qquad \boldsymbol{\gamma}_\mathrm{t}^{i,k+1}=0 \quad \forall i\in\mathcal{I}^k,$$

* Corresponding author: e-mail schroederbettina@hotmail.de, phone +00 491 769 247 527 5.
** e-mail kuhl@uni-kassel.de, phone +00 495 618 041 815, fax +00 495 618 043 631

(4)

$$\mathcal{A}_{\mathrm{t}}^{k+1} := \{i | \boldsymbol{\gamma}_{\mathrm{t}}^{i,k+1} + d\,\mathbf{r}_{2,\mathrm{t}}^{i,k+1} > 0\}, \quad \mathcal{I}_{\mathrm{t}}^{k+1} := \{i | \boldsymbol{\gamma}_{\mathrm{t}}^{i,k+1} + d\,\mathbf{r}_{2,\mathrm{t}}^{i,k+1} \leq 0\}, \quad d > 0,$$

where the incorporated matrices are extended properly. For a final solution a solver for linear systems of equations is applied.

4 Time Discretization Error Analysis for an Axisymmetric Model Problem

With the preceding procedure at hand, a time discretization error analysis for the axisymmetric benchmark problem of **Fig. 1**, where a time dependent sinusoidal load is applied to a cylinder with LAMÉ constants λ, μ, density ρ_0 and yield stress σ_y, is performed, cf. [4]. Hence, at the end of each time interval the global h-error of a quantity X is calculated by subtracting the numerically determined values X_{ns} from those obtained with a very small time step size $X_{ns}^{\Delta t/16}$, while identical initial values are taken into account. The local h-error estimator, however, is obtained, by performing two calculations with two distinct time step sizes simultaneously and comparing the results after each time step. Additionally, the results from the calculation using the bigger time step size are passed to the other one as initial condition for the next time step.

$$e_{ns}^{\mathrm{glob}} = ||X_{ns}^{\Delta t/16}(t_0) - X_{ns}(t_0)||, e_{ns} = ||X_{ns}^{\Delta t/2} - X_{ns}||, q^{\mathrm{loc/glob}} = \mathrm{mean}(\text{linear fit}(\log(\Delta t), \log(e_{ns}^{\mathrm{loc/glob}}))). \quad (5)$$

If these errors are determined for distinct time step sizes and collocated in vectors, expression $(5)_3$ can be used to determine the order of convergence of the time discretization scheme. A more detailed explanation is given in [4, 6] and references therein. For distinct RUNGE-KUTTA schemes the orders of convergence for different field variables, obtained from the local and the

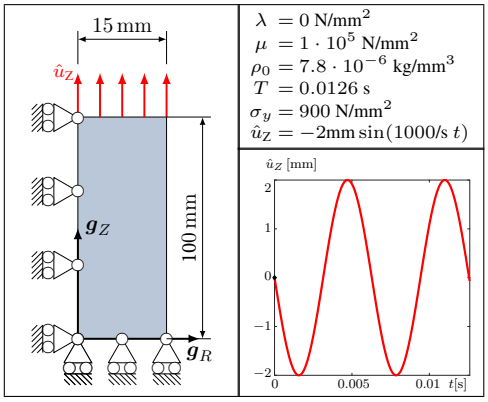

Fig. 1: Axisymmetric benchmark problem

Table 1: Estimation of the order of convergence

	$q^{\mathrm{loc}}(\boldsymbol{u})$	$q^{\mathrm{loc}}(\boldsymbol{\varepsilon}_{\mathrm{p}})$	$q^{\mathrm{loc}}(\boldsymbol{\sigma})$	$q^{\mathrm{glob}}(\boldsymbol{u})$	$q^{\mathrm{glob}}(\boldsymbol{\varepsilon}_{\mathrm{p}})$	$q^{\mathrm{glob}}(\boldsymbol{\sigma})$
LOBATTO IIIC(2)	1.54	1.51	1.38	1.89	1.76	1.22
LOBATTO IIIC(3)	3.76	3.87	3.65	2.33	2.34	2.84
RADAU IIA(2)	2.58	2.69	2.48	2.51	2.40	2.24
RADAU IIA(3)	4.77	4.98	4.71	2.22	2.19	2.48

global error, are shown in **Table 1**. Considering the local estimates, it becomes apparent that the Lobatto IIIC(2) method is quite far away from its theoretical order of two. In contrast, the Lobatto IIIC(3) scheme almost reaches its theoretical order of four for all considered field variables. A similar behavior can be recognized within the Radau IIA schemes. Analyzing the corresponding global measurements, however, yields a deviating picture. Apart from the Lobatto IIIC(2) scheme, all methods are estimated to reach orders well above two but not more.

5 Conclusion and Outlook

In the present paper the applicability of higher order accurate fully implicit RUNGE-KUTTA schemes to ideal elastoplasticity using a multifield approach is demonstrated. With the help of a model problem time discretization errors and the linked orders of convergence for distinct time integrators are compared. Orders of convergence of about five are obtained if the local h-error estimator is considered. But for the global h-error estimator an order of convergence greater than three could not be determined. An explanation for this order reduction phenomenon is still missing and hence an open task for further investigations.

Acknowledgements Open access funding enabled and organized by Projekt DEAL.

References

[1] J. C. Butcher, Numerical Methods for Ordinary Differential Equations. (John Wiley & Sons, 2008).
[2] C. Miehe, J Mech Phys Solids, **59**, p. 898-923.
[3] A. Popp, M. W. Gee, and W. A. Wall, Int J Numer Methods Eng, **79**, p. 1354-1391.

[4] B. Schröder, Consistent Higher Order Accurate Time Discretization Methods for Inelastic Material Models (kassel university press, 2019).
[5] K. Steinhoff, U. Weidig, and N. Saba, Investigation of Plastic Forming Under the Influence of Locally and Temporally Variable Temperature and Stress States, edited by K. Steinhoff, H. J. Maier, and D. Biermann, in: Functionally Graded Materials in Industrial Mass Production. (Verlag Wissenschaftliche Scripten, 2009), p. 353-364.
[6] K. Strehmel, R. Weiner, and H. Podhaisky, Numerik gewöhnlicher Differentialgleichungen. (Springer Spektrum, 2012).

